ISSN 0030-400X, Optics and Spectroscopy, 2017, Vol. 122, No. 3, pp. 504–509. © Pleiades Publishing, Ltd., 2017.
Original Russian Text © B.P. Aduev, D.R. Nurmukhametov, G.M. Belokurov, N.V. Nelyubina, A.V. Gudilin, 2017, published in Optika i Spektroskopiya, 2017, Vol. 122, No. 3, pp. 522–528.

LASERS AND THEIR APPLICATIONS

Spectral-Kinetic Characteristics of Luminescence of Pentaerythritol Tetranitrate with Inclusions of Iron Nanoparticles upon Explosion Induced by Laser Pulses

B. P. Aduev[a, *], D. R. Nurmukhametov[a], G. M. Belokurov[a], N. V. Nelyubina[a], and A. V. Gudilin[b]

[a] *Federal Research Center for Coal and Coal Chemistry, Siberian Branch, Russian Academy of Sciences, Kemerovo, 650000 Russia*

[b] *General Physics Institute of the Russian Academy of Sciences, Moscow, 119991 Russia*

**e-mail: lesinko-iuxm@yandex.ru*

Received June 6, 2016; in final form, September 8, 2016

Abstract—Spectral-kinetic characteristics of luminescence of tetranitropentaeritrite with inclusions of iron nanoparticles upon an explosion induced by laser pulses are measured with high temporal resolution. It is shown that the luminescence occurring during exposure to the laser pulse is a result of initiating a chemical reaction in tetranitropentaeritrite and is chemiluminescence. The glow is presumably associated with the excited nitrogen dioxide, NO_2, which is formed by the rupture of $O-NO_2$ bond in the tetranitropentaeritrite molecule.

DOI: 10.1134/S0030400X17020023

INTRODUCTION

In the early 1960s, there was interest in the development of detonators for initiating explosion by a laser pulse [1, 2], which possess several advantages compared with the currently used electric detonators, especially in terms of safety of performing blasting operations.

In this regard, there was a need for new materials with high sensitivity to laser irradiation and low sensitivity to mechanical shocks and electrical influences.

One of the directions of development of this work is the doping of brisant explosive with light-absorbing particles. The first works in this area were studies [3, 4], in which a significant effect of lowering the threshold for laser initiation of pentaerythritol tetranitrate (PETN) was achieved with the use of micron-sized light-absorbing additives.

Recently, several new results have been obtained in this field of research. It has been shown both theoretically and experimentally that the efficiency of light absorption by metal inclusions in PETN depends on the size and wavelength [5–7], while the decrease in the threshold of explosive decomposition is due to absorption of laser radiation by the inclusions and not due to an increase in the pathway of photons in the sample due to scattering, leading to an increase in light absorption by PETN [8–11]. Studies [12–14] reported experimentally determined minimum thresholds of explosive decomposition of PETN depending on the concentration of some metal inclusions, which significantly (by dozens of times) increase the sensitivity of the composites relative to PETN without inclusions.

Most researchers believe that light is absorbed by particles, which leads to their heating up to high temperatures ("hot spots"). This somehow triggers a self-sustaining chemical reaction leading to explosion of the sample [15–19]. The data needed for the explanation of the mechanisms of primary chemical transformations can be obtained by studying the spectral-kinetic characteristics of luminescence of the explosive substance with a high temporal resolution, which allows one to follow the processes from the moment when the substance in the condensed phase is exposed to a laser pulse.

The aim of this work is to study the spectral-kinetic characteristics of luminescence of PETN with inclusions of iron nanoparticles upon initiation of its explosion by a pulse of a neodymium laser.

EXPERIMENTAL

Explosion was initiated with the use of the first harmonic of a Nd:YAG laser (λ= 1064 nm) operating in the Q-switched mode. The duration of the laser pulse was τ = 14 ns and a maximum pulse energy was 1.5 J. The distribution of radiation intensity over the cross-section of the beam was close to rectangular. The

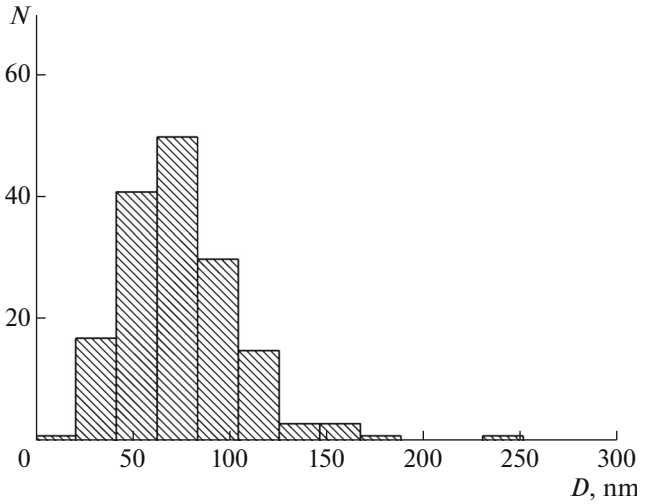

Fig. 1. Histogram of distribution of the iron-particle sizes.

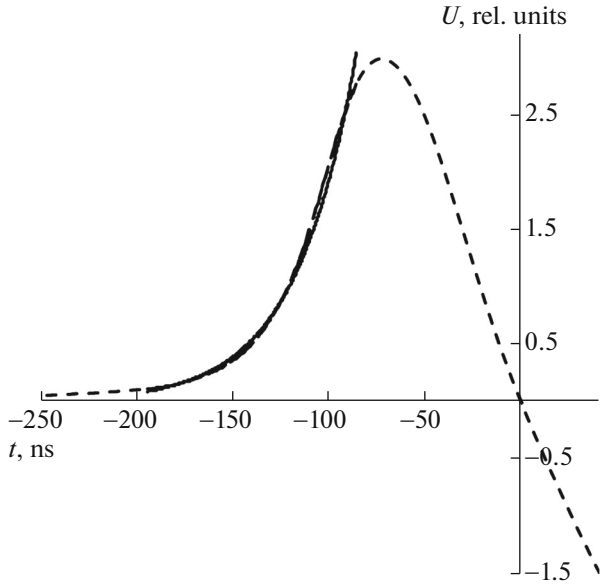

Fig. 2. Typical photoacoustic signal of a composite consisting of PETN with a 0.4% inclusion of iron particles. The broken curve is the recorded signal; the solid curve is its approximation by the exponential function.

exposure energy was regulated with the use of calibrated glass filters.

Experimental samples were prepared using a PETN powder with a narrow distribution of the particle sizes. The grain size at the distribution maximum was 1–2 μm. An iron powder prepared by the electroexplosive method[1] was used as the inclusion. The iron nanoparticles obtained by this method are coated with iron oxide II-FeO, which is resistant to further oxidation in air. Figure 1 shows the histogram of the particle-size distribution obtained from an image recorded with the use of a JEOL JSM 6390 LA electron microscope. As is seen from Fig. 1, the maximum of the particle-size distribution is at $d \approx 75$ nm. The content of iron and oxygen in the powder was determined using electron microprobe analysis; calculations of the FeO content yielded a value of 25% by weight. Assuming that the particles are spherical, an estimate of the oxide film thickness gave a value of ~5 nm.

The amount of Fe nanoparticles added to the PETN powder was 0.4% by weight. Experiments, discussion of which is beyond the scope of this work, showed that this concentration of inclusions allows achieving a minimum critical density of the energy of $H_{cr} = 0.5$ J/cm^2 corresponding to a 50% probability of explosion upon initiation by the first harmonic of the laser. The mixture was placed in hexane and stirred in an ultrasonic bath to obtain a uniform distribution of particles in the volume. After that, hexane was evaporated and the mixture was dried and separated to sample weights. The samples were prepared by pressing with the use of a hydraulic press and a special mold at the center of a 1-mm-thick copper plate that had a hole with a diameter of 3 mm for the sample. The density of the samples after pressing was $\rho = 1.7$ g/cm^3.

The extinction coefficient of the sample at the laser-radiation wavelength was measured by the optoacoustic method [20]. The sample was placed in acoustic contact with a piezoelectric detector and irradiated with a low-energy laser pulse (3 mJ) to avoid initiation of the chemical reaction. The acoustic response of the sample was converted into an electrical signal by the piezoelectric detector and recorded with a LeCroy WJ332A oscilloscope. The oscillogram is shown in Fig. 2.

The acoustic relaxation time of the sample [20],

$$\tau = (kc)^{-1}, \quad (1)$$

where k is the extinction coefficient and c is the speed of sound in the PETN ($c = 2500$ m/s) [11], was determined using the exponential part of the waveform. The measurements of the acoustic relaxation time gave a value of $\tau = 20$ ns, yielding a value of the extinction coefficient of $k = 200$ cm^{-1}. Consequently, the majority of the laser energy is adsorbed within an effective thickness of $x = k^{-1} = 50$ μm.

The plate with the sample was placed on an aluminum substrate and covered from the irradiated side with a plate made of optical glass with a thickness of 2 mm. The glass plate was covered with a copper plate with a hole at the center for radiation input. The copper plate with tightly pressed the glass plate to the sample surface the use of screws. The use of such a scheme allowed us to worsen the conditions of gas-dynamic

[1] The powder was prepared at Tomsk National Research University.

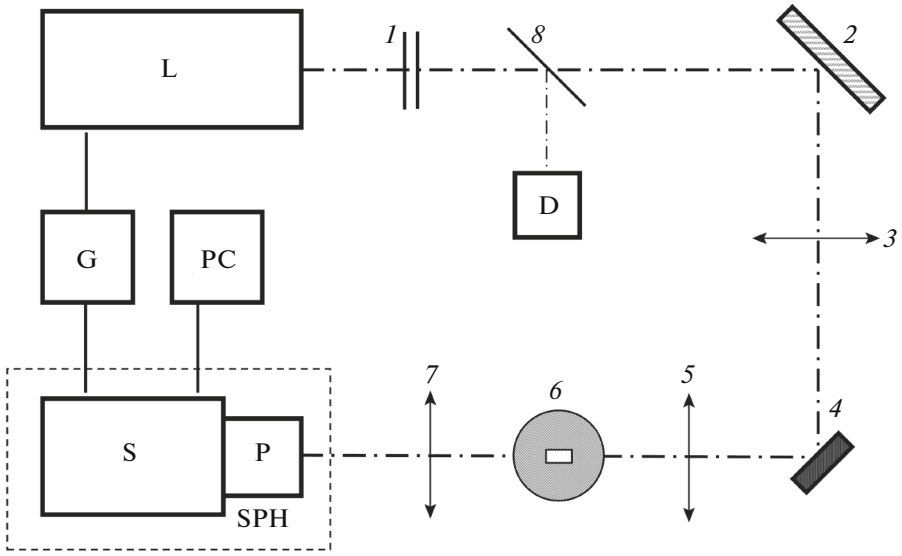

Fig. 3. Functional diagram of the experimental setup. (*1*) Neutral light filters, (*2*) mirror, (*3*) mirror lens (25 cm), (*4*) assembly with the studied sample, (*5, 7*) lenses (10 cm), (*6*) spatiotemporal slit (shown rotated by 90°), and (*8*) beam-splitting plate; L, pulsed Nd:YAG-laser; S, streak camera; P, polychromator; SPCh, VZGLYAD-2A spectrophotochronograph; G, synchronization unit; PC, computer; and D, photodiode.

relief, which leads to a decrease in the threshold of explosive decomposition.

A functional diagram of the setup is shown in Fig. 3. Laser radiation L is attenuated by neutral filters *1* and, with the use of rotary mirror *2* and lens *3* (F = 25 cm), is focused on assembly *4* with the studied sample. Assembly *4* is positioned at an angle of 45° to the laser beam and the optical axis of the measuring system. As a result of such geometry, the irradiated spot on the sample surface is an ellipse with axes of 2 and 2.8 mm with irradiation of the copper plate being excluded.

With the help of lens *5*, the image of the sample is formed in the plane of spatiotemporal slit *6*. The hole in the slit has dimensions of 0.2 × 0.1 mm and defines the spectral and temporal resolutions of the recording system, 10 nm and 2 ns, for the scan of streak-camera *S* shown in Fig. 5 and 10 ns in Fig. 4. With the help of lens *7*, the image of the spatiotemporal slit is transmitted to the input of polychromator P. The strip of the spectrum at the polychromator output was swept in time with the use of a photochronograph on the basis of an electro-optical converter (EOC) operating in the linear scan mode (a streak-camera). As a single unit, photochronograph S and polychromator P represent a VZGLYAD-2A spectrophotochronograph (SPCh) (LLC Scientific and Special Precision Instruments and Systems, Moscow). The light matrix from the output screen of the EOC is read by a CCD sensor and transmitted to a storage device of a PC for further digital processing. A G5-56 G pulse generator is used for triggering the laser and the time-sweep of the streak camera.

The recorded signal forms a matrix, the vertical elements of which allows one to obtain the luminescence spectrum of the sample in the 350–750 nm range, while the horizontal elements are used to obtain

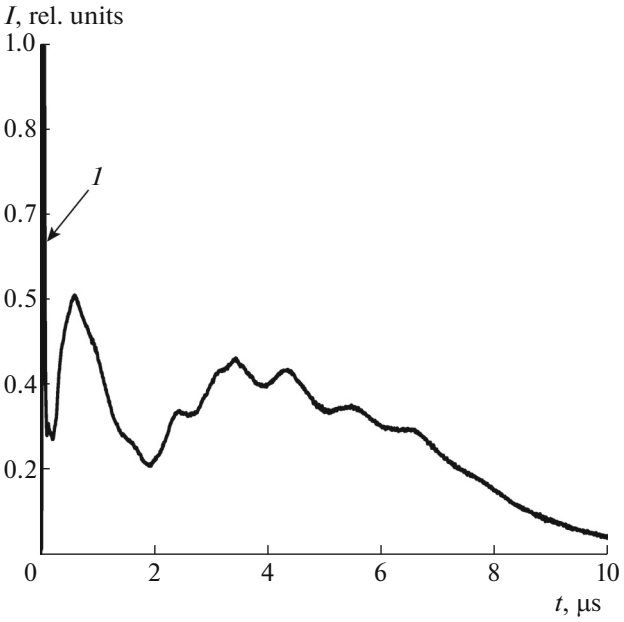

Fig. 4. Overview of the kinetics of the luminescence arising upon explosion of the sample. *1* is the maximum of the luminescence occurring at the moment of impact of the laser pulse. The density of the laser-radiation energy is 1.3 J/cm^2.

kinetics of the sample luminescence at a selected wavelength within the specified spectral range.

To obtain the "true" luminescence spectrum of the sample, we used the reference lamp method [21]. The reference lamp was a TRS 2850-3000. Its spectrum was recorded in the time-sweep mode. The "true" spectrum of the lamp can be calculated by the Planck formula with the use of the known color temperature (taking into account the grayness coefficient of tungsten). The sensitivity of the registration system at the given point of the spectrum is determined by dividing the measured intensity by the calculated value. The "true" spectrum is obtained by dividing the recorded intensity of the sample luminescence by the sensitivity at the corresponding points of the spectrum at a given moment of time or at different time moments at the given wavelength.

RESULTS AND DISCUSSION

Figure 4 shows an overview of kinetics of luminescence arising from a sample explosion. The first luminescence peak occurs upon exposure to the laser pulse, when the sample is still in the condensed phase. The luminescence in the microsecond range results from the reaction of explosive decomposition of the sample and is associated with gaseous products.

Because the aim of this work is the study of the initial stage of the reaction in the condensed phase, we will discuss below the spectra and kinetics of the first peak in Fig. 4 measured in a shorter time domain using a spectrophotochronograph (SPCh in Fig. 3).

Figure 5 shows the luminescence spectra at the time moment of the end of the laser pulse and at different energy densities: close to the threshold of explosive decomposition ($H_{cr} = 0.7$ J/cm^2, Fig. 5a), exceeding the threshold by ~2.5 times ($H_{cr} = 1.3$ J/cm^2, Fig. 5b), and exceeding it by five times ($H_{cr} = 2.5$ J/cm^2, Fig. 5c). As can be seen from Fig. 5, the shape of the spectrum significantly depends on the energy of the pulse-initiator. An increase in the initiation energy leads to an increase in the luminescence intensity in the short-wavelength part of the spectrum. The form of the spectrum does not change relative to Fig. 5c as the intensity of the laser pulse is further increased up to 5 J/cm^2.

The kinetics of the luminescence at two wavelengths is shown in Fig. 6. The luminescence intensity drops to a minimum value in the course of ~150 ns and in some cases has a nontrivial nature in the range of 500–540 nm.

The spectra in Fig. 5 cannot be described by the Planck formula and, therefore, the origin of the luminescence is not thermal. It appears very unlikely that there is multiphoton absorption of laser radiation (three to four quanta) leading to laser-induced luminescence, since the probability of such a process is low

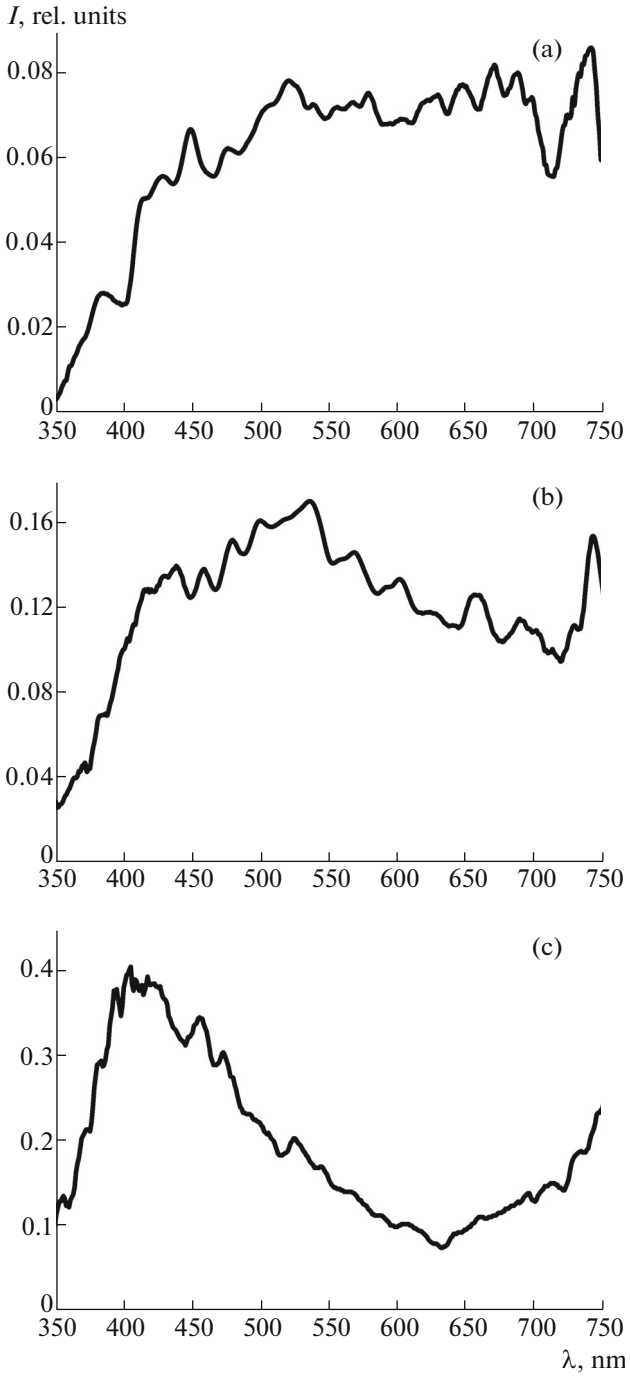

Fig. 5. Spectra of luminescence at the time moment corresponding to the end of the laser pulse at different densities of the laser-radiation energy: (a) 0.7, (b) 1.3, and (c) 2.5 J/cm^2.

and the samples without inclusions show no luminescence for this density of the laser energy. Therefore, the heating of the inclusions upon absorption of the laser radiation plays a key role; according to theoretical calculations, heating should reach a temperature of $T > 1000$ K [18]. Due to the heat transfer during the

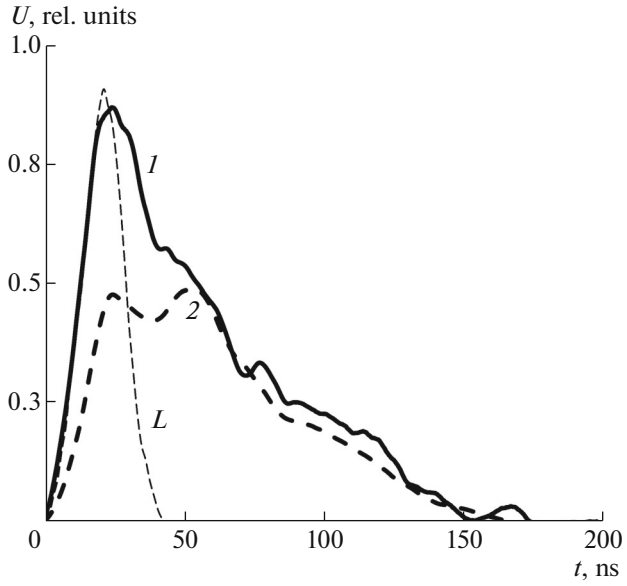

Fig. 6. Kinetics of luminescence at different wavelengths: (*1*) 420 and (*2*) 530 nm. The density of the laser-radiation energy is 2.5 J/cm^2. L is the laser pulse.

laser pulse, the shell around the inclusion should warm up, reaching the same temperature as the temperature on the inclusion surface [18, 19].

Shell thickness d can be estimated as

$$d = (\chi\tau_i)^{1/2}, \quad (2)$$

where $\chi = 1.1 \times 10^{-3}$ cm^2/s is the thermal diffusivity coefficient of PETN and $\tau = 14$ ns is the duration of the laser pulse.

The calculation yields a value of $d = 40$ nm. Thus, a layer of PETN around the inclusion is heated up above the melting temperature ($T_m = 414$ K) apparently already at the front edge of the laser pulse. This creates conditions for initiation of an exothermic chemical reaction in the PETN layer surrounding the nanoparticle. As a result, excited fragments of PETN molecules are formed during the time of the laser pulse. Luminescence of some fragments is observed in the studied spectral range.

Thus, the main result of the presented study is the conclusion that the luminescence occurring during impact of the laser pulse is chemiluminescence. Emitting particles should be looked for among the small molecules which are formed upon decomposition of the PETN molecule and have a small number of degrees of freedom compared to large fragments.

Analysis of literature data suggests that the observed luminescence is likely due to excited nitrogen dioxide NO_2 which is formed upon rupture of the O–NO_2 bond in the PETN molecule. This suggestion is based on the following literature data.

Luminescence of NO_2 upon exposure to light with $\lambda > 380$ nm spans the region from the excitation wavelength and up to 7500 Å and above. The continua are superimposed with a large number of rotational and vibrational lines [22].

Upon excitation at $\lambda = 435.8$ nm, luminescence of NO_2 spans the range from the excitation wavelength up to 700 nm with a maximum at 520 nm [23]. The laser-induced luminescence of NO_2 at excitation wavelengths of 460, 532, 560, 584, and 640 nm was studied in [24]. In all cases, luminescence was observed in the region from the excitation wavelength up to the long-wavelength limit of the registration system at $\lambda = 850$ nm; the maximum of the luminescence intensity was observed with a shift of ~100 nm from the excitation wavelength [24]. The above literature data indicate that the shape of the NO_2 luminescence spectrum depends on the degree of excitation of the molecule, i.e., on the filling of the vibrational–rotational levels of the excited state.

This explains the different forms of the luminescence spectra in Fig. 3 depending on density of initiation energy H. With increasing H, the temperature of the "hot spot," which is a nanoparticle with the PETN shell surrounding it, grows during the laser pulse. This leads to an increase in the level of the initiating chemical reaction in the heated PETN shell and the temperature of the reaction fragments, resulting in an increase in the degree of filling of the vibrational–rotational levels of the excited state of NO_2. The result is the change in the shape of the spectra with increasing luminescence intensity in the short-wavelength region of the spectrum.

Note that, for the spectral maximum at $\lambda = 420$ nm, no shift to shorter wavelengths is seen as H increases from 2.5 to 5 J/cm^2. This may indicate complete filling of the vibrational–rotational levels of the excited state, because, as the excitation energy increases, the molecule dissociates, $NO_2 \rightarrow NO + O$, when the energy transferred to the molecule is ≥3.11 eV [25].

Considering the process in general, we note that, according to the kinetic curve in Fig. 4, the chemical reaction propagates from the region of the hot spots and, in the ~0.5–5 μs region, there is growth in the intensity of luminescence, in which the component from the blast plasma already becomes dominant.

CONCLUSIONS

1. It is shown that the chemical reaction in the PETN + iron nanoparticles composite begins immediately during the initiating laser pulse.

2. Excited NO_2 molecules luminescing in the 350–750 nm spectral range are one of the primary products of the reaction.

3. The development of the chemical reactions in the microsecond time interval leads to explosive decomposition of the sample.

REFERENCES

1. T. H. Maiman, Nature **187** (4736), 1038 (1960).
2. A. Javan, W. R. Bennett, and D. R. Herriott, Phys. Rev. Lett. **6**, 106 (1961). doi 10.1103/PHYSREVLETT.6.106
3. V. B. Ioffe, A. V. Dolgolaptev, V. E. Aleksandrov, and A. P. Obraztsov, Combust., Explos., Shock Waves **21** (3), 316 (1985). doi 10.1007/BF01463849.
4. V. E. Aleksandrov, A. V. Dolgolaptev, and V. B. Ioffe, Combust., Explos., Shock Waves **19** (4), 384 (1983). doi 10.1007/BF00783625.
5. B. P. Aduev, D. R. Nurmukhametov, A. A. Zvekov, and I. Yu. Liskov, Combust., Explos., Shock Waves **51**, 472 (2015). doi 10.1134/S0010508215040115
6. B. P. Aduev, D. R. Nurmukhametov, R. I. Furega, A. A. Zvekov, and A. V. Kalenskii, Russ. J. Phys. Chem. B **7**, 453 (2013). doi 10.1134/S199079311304012X
7. A. V. Kalenskii, A. A. Zvekov, A. P. Nikitin, M. V. Anan'eva, and B. P. Aduev, Opt. Spectrosc. **118**, 978 (2015). doi 10.1134/S0030400X15060119
8. B. P. Aduev, D. R. Nurmukhametov, G. M. Belokurov, and R. I. Furega, Combust., Explos., Shock Waves **51**, 347 (2015). doi 10.1134/S0010508215030107
9. B. P. Aduev, D. R. Nurmukhametov, A. A. Zvekov, A. P. Nikitin, N. V. Nelyubina, G. M. Belokurov, and A. V. Kalenskii, Instrum. Exp. Tech. **58**, 765 (2015). doi 10.1134/S0020441215050012
10. B. P. Aduev, D. R. Nurmukhametov, G. M. Belokurov, A. A. Zvekov, A. V. Kalenskii, A. P. Nikitin, and I. Yu. Liskov, Tech. Phys. **59**, 852 (2014). doi 10.1134/S1990793114110128
11. B. P. Aduev, D. R. Nurmukhametov, R. I. Furega, and I. Yu. Liskov, Russ. J. Phys. Chem. B **8**, 852 (2014). doi 10.1134/S1990793114110128
12. B. P. Aduev, D. R. Nurmukhametov, R. I. Furega, and A. A. Zvekov, Russ. J. Phys. Chem. B **8**, 352 (2014). doi 10.1134/S1990793114030178
13. B. P. Aduev, G. M. Belokurov, D. R. Nurmukhametov, and N. V. Nelyubina, Combust., Explos., Shock Waves **48**, 361 (2012). doi 10.1134/S001050821203015X
14. B. P. Aduev, D. R. Nurmukhametov, and R. V. Furega, Solid Fuel Chem. **46**, 371 (2012). doi 10.3103/S036152191206002X
15. N. K. Bourne, Proc. R. Soc. London A **457**, 1401 (2001). doi 10.1098/RSPA.2000.0721
16. V. A. Arkhipov and A. G. Korotkikh, Combust. Flame **159**, 409 (2012). doi 10.1016/J.COMBUSTFLAME.2011.06.020
17. Y. Yang, Z. Sun, S. Wang, and D. Dlott, J. Phys. Chem. B **107**, 4485 (2003). doi doi 10.1021/JP0269322
18. B. P. Aduev, M. V. Anan'eva, A. A. Zvekov, A. V. Kalenskii, V. G. Kriger, and A. P. Nikitin, Combust., Explos., Shock Waves **50**, 704 (2014). doi 10.1134/S0010508214060112
19. A. V. Kalenskii, M. V. Anan'eva, A. A. Zvekov, and I. Yu. Zykov, Tech. Phys. **60**, 437 (2015). doi 10.1134/S1063784215030081
20. V. E. Gusev and A. A. Karabutov, *Laser Opto-Acoustics* (Nauka, Moscow, 1991; AIP, New York, 1993).
21. L. V. Levshin and A. M. Saletskii, *Luminescence and its Measurements* (Mosk. Gos. Univ., Moscow, 1989) [in Russian].
22. H. Okabe, *Photochemistry of Small Molecules* (Wiley, New York, 1978).
23. G. H. Myers, D. M. Silver, and F. Kaufman, J. Chem. Phys. **44**, 1063 (1966). doi 10.1063/1.1726751
24. D. Oh, S. Sisk, A. Young, and H. Johnston, J. Chem. Phys. **85**, 1063 (1986). doi 10.1063/1.451348
25. V. Kurkal, P. Fleurat-Lessard, and R. Schinke, J. Chem. Phys. **119**, 1063 (2003). doi 10.1063/1.1580475